

Investigation of hydrazine electrooxidation performance of carbon nanotube supported Pd monometallic direct hydrazine fuel cell anode catalysts

Omer Faruk Er,¹ Ali Cavak,¹ Adnan Aldemir,¹ Hilal Kivrak^{1,*}

¹ Van Yuzuncu Yil University, Faculty of Engineering, Department of Chemical Engineering, Van 65000, Turkey, hilalkivrak@yyu.edu.tr, hilalkivrak@gmail.com, ORCID: 0000-0001-8001-7854

ABSTRACT

In this study, carbon nanotube (CNT) supported Pd/CNT catalysts at varying Pd molar ratios (Pd involving among 0.1-20 wt %) are prepared via NaBH₄ reduction method. The surface of catalysts prepared for hydrazine electrooxidation are successfully characterized via N₂ adsorption-desorption measurements, X-ray diffractometer (XRD), X-ray photoelectron spectroscopy (XPS), and transmission electron microscope (TEM). Electrochemical measurements are performed using cyclic voltammetry (CV) and electrochemical impedance spectroscopy (EIS) techniques. According to the characterization results, for 5% Pd/CNT catalyst, the average particle size and the surface area are determined as 5.17 nm and 773.10 m² g⁻¹, respectively. Among Pd containing (0.1-20 wt %) CNT supported catalysts, 5%Pd/CNT catalyst exhibits the best current density as 6.81 mA cm⁻² (1122.63 mA mg⁻¹ Pd). Furthermore, 5% Pd/CNT catalyst shows the best charge transfer resistance (R_{ct}) compared to Pd/CNT catalysts. Pd/CNT catalysts are promising anode catalysts for direct hydrazine fuel cells.

ARTICLE INFO

Research article

Received: 28.09.2020

Accepted: 17.12.2020

Keywords:

Pd,
CNT,
hydrazine,
electrooxidation,
direct hydrazine fuel
cell,
anode

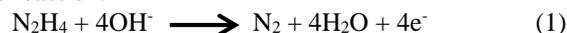
*Corresponding author

1. Introduction

The demand for energy, in which the vast majority of this demand is provided from fossil fuel is constantly increasing in the industrialized world [1, 2]. The use of fossil fuels that caused global warming and environmental pollution is constituted negative consequences for both nature and human life [3]. Fuel cell technologies could be employed to supply energy to cover the energy demand instead of fossil fuels [4].

Recently, the most commonly used fuels in fuel cell technology are hydrazine, formic acid [5], ethanol [6], methanol [7], glucose [8], and ethylene glycol [9] etc. Hydrazine is a preferable fuel due to its superior properties such as high energy density, low cost, zero CO₂ emission, convenient storage, and transportation ease [10, 11]. In addition, another feature of hydrazine is that its source (H₂ and N₂) is unlimited in nature. Hydrazine is not explosive and it has low toxicity in dilute aqueous solutions [11]. In direct hydrazine fuel cells (DHFC), catalyst poisoning products such as CO do not release, so the overvoltage of catalyst poisoning is low in DHFC [12]. Anode, cathode, and overall reaction of hydrazine electrooxidation are given as follows [13, 14]:

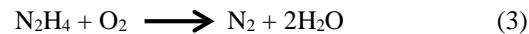
Anodic reaction:



Cathodic reaction:



Overall reaction:



As a result of reactions (1-3) occurring in the oxidation of hydrazine, only water and nitrogen are formed as products, and these products are released into the environment [15].

There are needs for low cost and more efficient catalysts with higher catalytic activity in hydrazine fuel cells. For this purpose, PtCu/C [16], P-Cu₂Ni/C [17], NiCoP/C [18], SeNCM [19], Ni₃S₂@Ni foam [20], Mn₂O₃-Fe₂O₃/CFs [21], Ni-Pt/C [22], nano-CuO/MGCE [23], Ni₃N nanoparticles [24], Co_{fiber}/Cu [25], Ni₂P@Ni₁₀Mo/Ni-Mo-O/NF [26], and Ni foam@Ag-Ni [27] catalysts were studied in DHFC for catalysts with low costs and higher catalytic activity. In addition, Yang et al. stated that the Ag/CNT catalyst prepared by modification Ag nanoparticles on CNT with benzyl

mercaptan showed high catalytic activity the hydrazine electrooxidation reaction [28]. In another study, Gao et al. remarked that Cu nanotube-graphene paper (Cu-GP) electrode developed by the facile electrodeposition method had high electrocatalytic activity and durability for DHFC in alkaline medium [29]. Furthermore, Asset et al. reported that NiMo/C catalyst prepared via wet impregnation process method, exhibited better catalytic activity compared to Ni/C catalyst

[30]. Liu et al. reported that the ternary CuNiCo LDH nanosheet array catalyst prepared via sulfurization-induced edge amorphization exhibited good catalytic activity and power durability[31]. The catalysts and maximum peak values compiled from the literature studies for hydrazine electrooxidation were given in Table 1.

Table 1: Catalysts and maximum peak values for hydrazine electrooxidation compiled from literature.

Catalyst	Preparation	Maximum Peak mA cm ⁻²	Reference
Pd black	---	4.12	[32]
Pd NCs	---	4.87	[32]
AuPd NCs	simple one-pot successive co-reduction	5.28	[32]
AuPd DANCs	simple one-pot successive co-reduction	9.57	[32]
Co@NM	electrochemical deposition	8.13	[33]
VGNH-45	scalable plasma-enhanced chemical vapor deposition	13	[34]
Bulk Au electrode	---	0.9	[35]
NPGL30	etching 12-carat white gold leaves	10.5	[35]
MnO/N-C	---	6.3	[36]
Pd/CNT	NaBH ₄ reduction	6.81	In this study

In this study, Pd/CNT catalysts were prepared at varying Pd weight loadings via NaBH₄ reduction method. The electrochemical performances of prepared catalysts were investigated via CV and EIS. These catalysts were characterized with advance surface characterization methods as XRD, XPS, and TEM to describe the surface chemical and physical properties. The particle size and the crystal structure of synthesized catalysts were determined via XRD and TEM.

2. Experimental measurement

2.1. Materials and Equipment

Potassium tetrachloropalladate (II) (K₂PdCl₄, 99.99%), Hydrazine (NH₂NH₂, 98%) sodium borohydride (NaBH₄, 99%), multi-walled carbon nanotube (MWCNT, 98%), KOH were purchased from Sigma-Aldrich and used as received. Nafion 117 solution (5%) was supplied from Sigma-Aldrich. Ag/AgCl reference electrode and Pt wire electrodes used in potentiostat were purchased from CH Instruments. Deionized water was distilled via water purification system (Milli-Q Water Purification System). All glass wares were washed with acetone and a wealth of rinsed with distilled water.

2.2. Preparation of catalysts and working electrodes

2.2.1. Synthesis of Pd/CNT catalysts

Pd/CNT catalysts were prepared by NaBH₄ reduction method. Pd metal precursor (Potassium tetrachloropalladate) was completely dissolved in pure water and then CNT was added. These mixtures were stirred in ultrasonic bath for two hours.

NaBH₄ was added to this mixture to reduce the salts in the medium. After the addition of NaBH₄, these mixtures were stirred in the ultrasonic bath for one hour and filtered. These catalysts were completely dried at 85 °C for 12 hours.

2.2.3 Preparation of working electrodes

The working electrode (glassy carbon electrode) was firstly polished by alumina. 3 mg of catalyst was distributed homogenously in 1 mL of 5% Nafion solution. Consequencely, a catalyst ink was obtained. Finally, 3 µl of catalyst ink was dropped on a working electrode and the electrode was dried at room temperature to remove the solvent.

2.3. Metal Characterization Techniques

Pd/CNT catalysts were characterized via N₂ adsorption-desorption, XRD, XPS, and TEM. Surface areas were measured through Micromeritics 3Flex equipment. The Pd diffractions on the surface that 5% Pd/CNT of the best ratio of these catalysts were determined using XRD. Particle size and surface metal distribution were found via TEM.

2.4. Electrochemical Measurements

All electrochemical measurements of Pd/CNT catalysts were determined by CV and EIS in 1 M KOH + 0.5 M N₂H₄ solution. These measurements were obtained using the three-electrode system in potentiostat CH660E. The electro-oxidation activities of these catalysts were performed by CV at the potential gap of -1.2 V to 0.8 V at 50 mv s⁻¹ scan rate. The electrochemical impedances of these catalysts were

obtained with EIS at 316 kHz and 0.046 Hz to 5 mV amplitude.

3. Results and discussion

3.1. Physical characterization

5% Pd/CNT catalyst was characterized by BET, XRD, XPS, and TEM. Fig. 1 shows the N_2 adsorption-desorption isotherm and XRD pattern of monometallic 5% Pd/CNT catalyst prepared via $NaBH_4$ reduction method. 5% Pd/CNT catalyst exhibited V-type adsorption-desorption shape with H1 type hysteresis loop (Fig. 1a) [5, 37]. Adsorption-desorption hysteresis loop is close to mesoporous pore structure. The average particle size, pore size, and pore volume of 5% Pd/CNT catalyst were found at 7.76 nm, 11.35 nm, $2.08 \text{ cm}^3 \text{ g}^{-1}$, respectively. Furthermore, BET surface area of 5% Pd/CNT was calculated as $773.10 \text{ m}^2 \text{ g}^{-1}$.

The XRD pattern of monometallic Pd/CNT catalyst is given in Figure 1b. It is found that the C (0 0 2) plane, which related to reflection of hexagonal carbon structure, diffraction peak located towards 25.6° [38]. The (1 1 1), (2 0 0), (2 2 0), and (3 1 1) planes, which shows face center cubic (fcc), belonging to Pd the diffraction peaks are subtended of 2θ values at 39.2° , 45.4° , 66.6° , and 79.7° , respectively [39]. In addition, Pd (1 1 0) diffraction peak was seen at 42.8° [40]. The crystal size for 5% Pd/CNT catalyst was calculated as 6.94 nm with the Scherrer's equation.

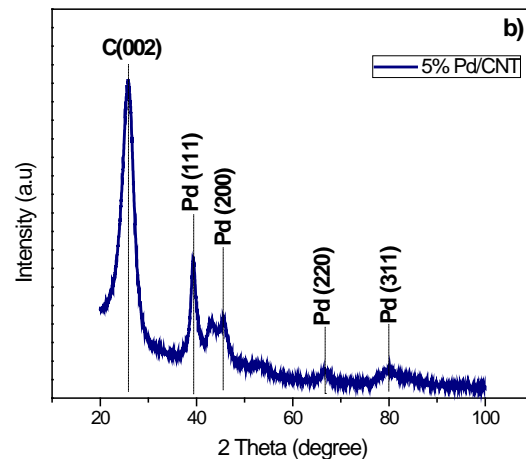
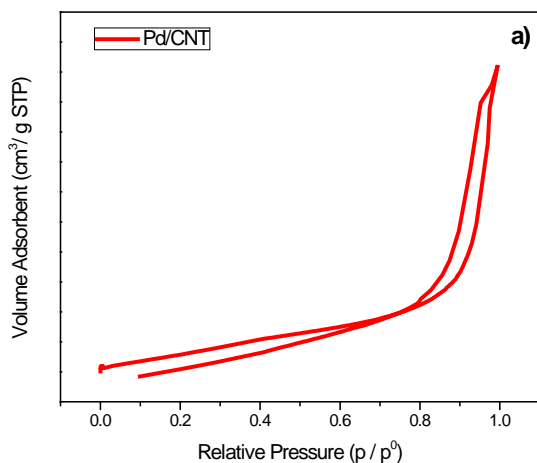


Figure 1. a) N_2 adsorption-desorption isotherm and b) XRD pattern of the monometallic 5% Pd/CNT catalyst.

Atomic differences on the CNT surface could be easily determined via XPS analysis [41]. The oxidation state of the Pd on CNT surface was determined by XPS analysis. Here, according to C 1s, which found at 284.4, was determined the binding energy of Pd (Fig. 2b). XPS spectra of Pd 3d, C 1s, O 1s, and general survey were given in Fig. 2 and the oxidation state of Pd 3d is presented in Table 2 for 5% Pd/CNT catalyst. The resolution of Pd 3d spectra was found for Pd^0 ($3d_{5/2}$ 335.6 eV; $3d_{3/2}$ 341.9 eV) and Pd^2 (PdO_2 339.0 eV) (Fig. 2a and Table 2). In addition, the undefined spectrum was seen at 351.2 eV that could be impurity remaining from the synthesis method (Table 2). The elemental state of Pd^0 on CNT surface was determined at relative density as 49.4 (Table 2). TEM was used to determine the particle size and morphological structure of 5% Pd/CNT catalyst. TEM images and particle size histogram of 5% Pd/CNT catalyst is given in Fig. 3. It is clearly seen that Pd nanoparticles were bonded with the exterior surface of CNT. Furthermore, from Fig. 3(b and c), one could note that Pd nanoparticles aggregated. In addition, Pd nanoparticles distributed homogeneously on the surface of CNT. It was found that the average particle size of 5% Pd/CNT catalyst as 5.17 nm (Fig. 3(f)).

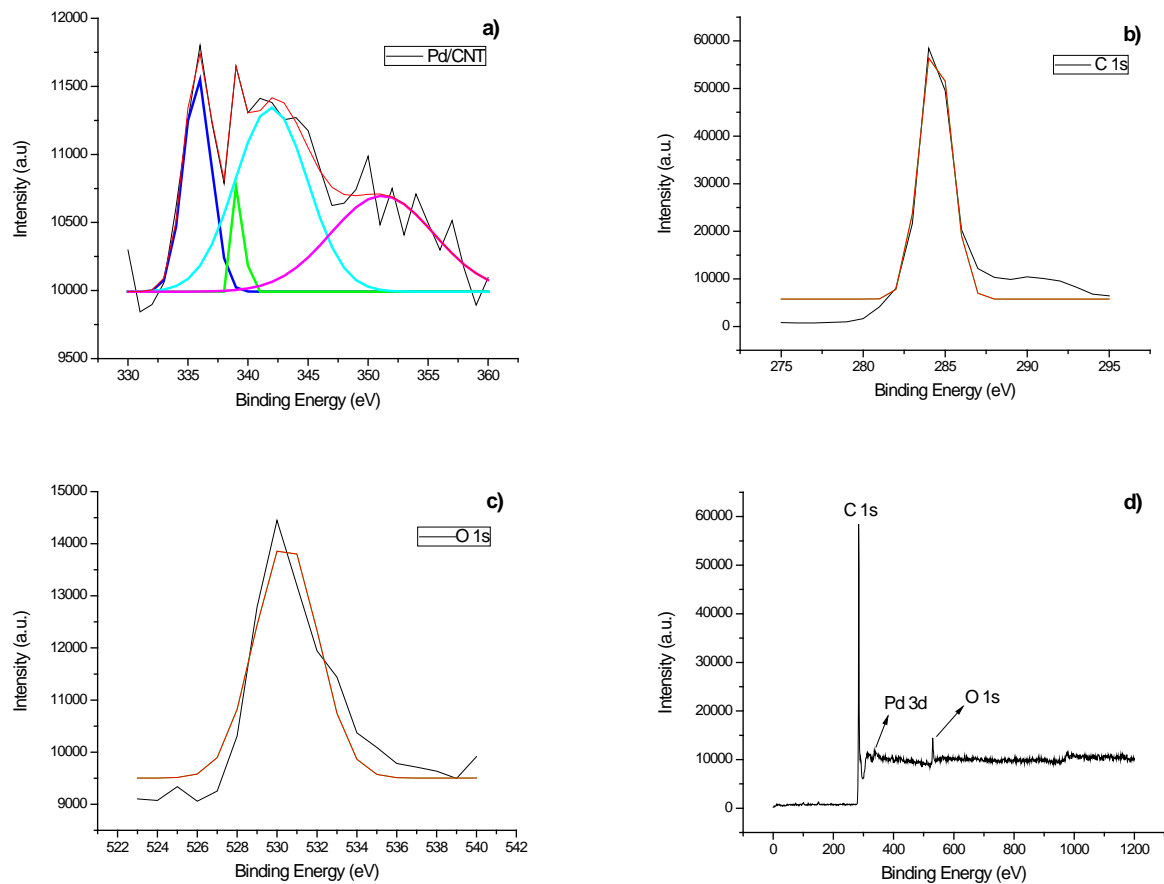


Figure 2. XPS spectra of a) Pd 3d, b) C 1s, c) O 1s, and d) general survey of Pd/CNT catalyst.

Table 2. Pd 3d binding energy of Pd/CNT electro-catalysts.

Catalyst	Species	Binding Energy (eV)	Possible Chemical State	Relative Intensity (%)	Reference
Pd/CNT	Pd 3d	335.6	Pd 3d _{5/2} (Pd ⁰)	24.5	[42]
		339.0	PdO ₂	24.7	[43]
		341.9	Pd 3d _{3/2} (Pd ⁰)	24.9	[42]
		351.2	Undefined	25.6	

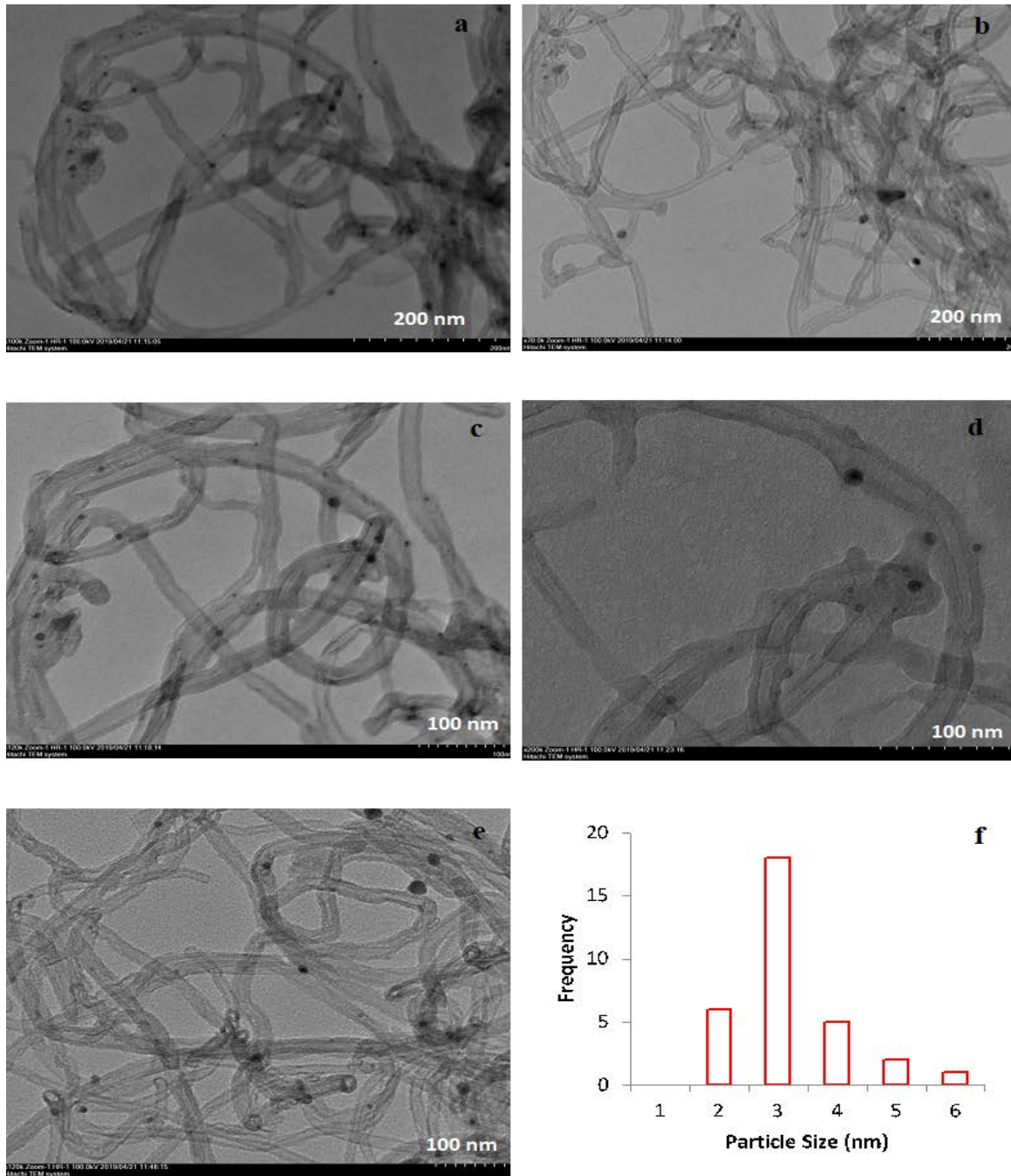


Figure 3. TEM images (a, b, c, d, and e) and particle size (f) of 5% Pd/CNT.

3.2. Electrochemical assessment

CV and EIS measurements were taken in 1 M KOH + 0.5 M N_2H_4 solution to determine hydrazine oxidation activities of Pd/CNT supported catalysts prepared at (0.1-20 wt %) Pt loadings via $NaBH_4$ reduction method. Initially, CV measurements of prepared catalysts were taken in 1 M KOH solution and in 1 M KOH + 0.5 M N_2H_4 solution at -1.0 V to 0.4 V potentials a scan rate of 50 mV s^{-1} , respectively. These results were presented in Fig. 4 and Table 3. The hydroxide

(OH^-) adsorption-desorption peak was observed at among -0.4 V and 0.2 V for 0.1% Pd/CNT catalyst, but this peak was observed at -0.3 V and 0.2 V for 5% Pd/CNT catalyst (Fig. 4(a)). This could be explained by the fact that Pd nanoparticles are very well dispersed on the CNT surface, and thus lead to more OH^- adsorption. As seen, OH^- electrooxidation peaks for all prepared catalysts were seen. After reducing the surface oxidation of the catalyst, more Pd active sites were provided for adsorption and oxidizing the hydrazine. 5% Pd/CNT

catalyst among the prepared catalysts showed the highest performance as 6.81 mA cm⁻² (1122.63 mA mg⁻¹ Pd) for hydrazine electrooxidation (Fig. 4(b) and Table 3). In addition, the forward currents (I_f) and reverse currents (I_r) of these catalysts were studied. After evaluation of these results, we concluded that 5% Pd/CNT catalyst had the best activity for hydrazine electrooxidation (Table 3).

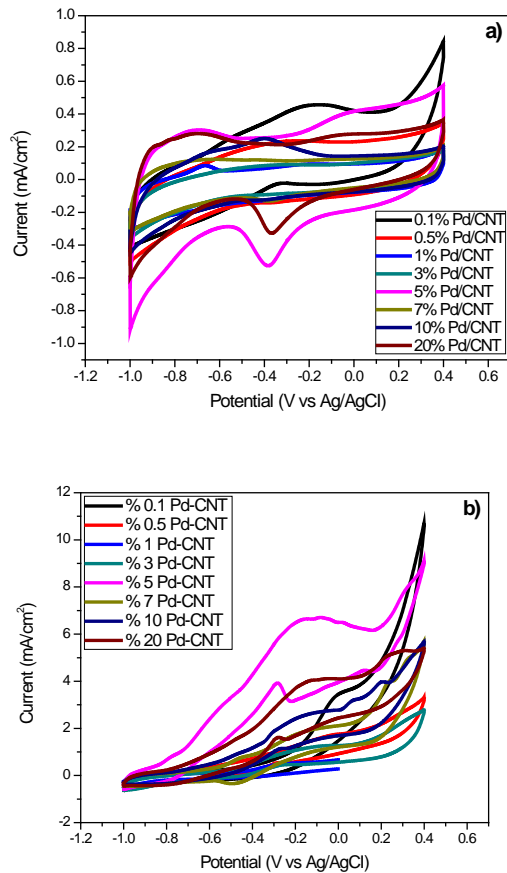


Figure 4. Cyclic voltammograms with a 50 mV s⁻¹ scan rate in a) 1 M KOH solution on Pd/CNT catalysts and b) 1 M KOH + 0.5 M N₂H₄ solution on Pd/CNT catalysts.

Table 3. Properties of the obtained peaks from CV results

Catalysts	Forward Peak		Reverse Peak		I _f /I _r	Peak Current Density (mA cm ⁻²)
	I _f (mA cm ⁻²)	E (V)	I _r (mA cm ⁻²)	E (V)		
0.1% Pd/CNT	3.86	0.020	---	---	---	3.57
0.5% Pd/CNT	2.31	-0.004	1.12	-0.26	2.06	1.76
1% Pd/CNT	0.77	-0.203	0.24	-0.70	3.20	0.54
3% Pd/CNT	1.74	-0.015	1.10	-0.21	1.58	1.23
5% Pd/CNT	7.35	-0.081	4.40	-0.28	1.67	6.81
7% Pd/CNT	2.36	-0.047	1.42	-0.58	1.66	2.10
10% Pd/CNT	3.12	-0.031	2.02	-0.05	1.54	2.77
20% Pd/CNT	4.55	-0.031	2.06	-0.27	2.21	4.14

EIS method is the best method to investigate in a large variety of catalyst properties [44]. Nyquist plots were obtained at different potentials for 5% Pd/CNT catalyst and at 0.4 V for different percent Pd/CNT catalysts and presented in Figure 5. The Nyquist Plots obtained from EIS measurements were taken in 1 M KOH + 0.5 M N₂H₄ solution. The Nyquist Plots are shaped usually as semicircle. These diameters of semicircles that correlate with charge transfer resistance (R_{ct}) could inform about the electrocatalytic activity of catalysts [45]. The smaller the diameter of the semicircles, the charge transfer resistance of the catalyst is smaller, which specified the high electrocatalytic activity of the catalyst. Thus, more the hydrazine electrooxidation reaction gets faster. From the measurements taken at different potentials on 5% Pd/CNT catalyst at 0.4 V, we observed that this catalyst displayed the best catalytic activity in hydrazine electrooxidation reaction (Fig. 5a). Furthermore, in the measurements taken at 0.4 V, it is found that among the Pd/CNT catalysts, 5% Pd/CNT catalyst possess the best the charge transfer resistance in hydrazine electrooxidation reaction (Fig. 5b). This could be explained by the fact that Pd nanoparticles are well distributed on the CNT surface and leads to oxidation of more hydrazine molecules.

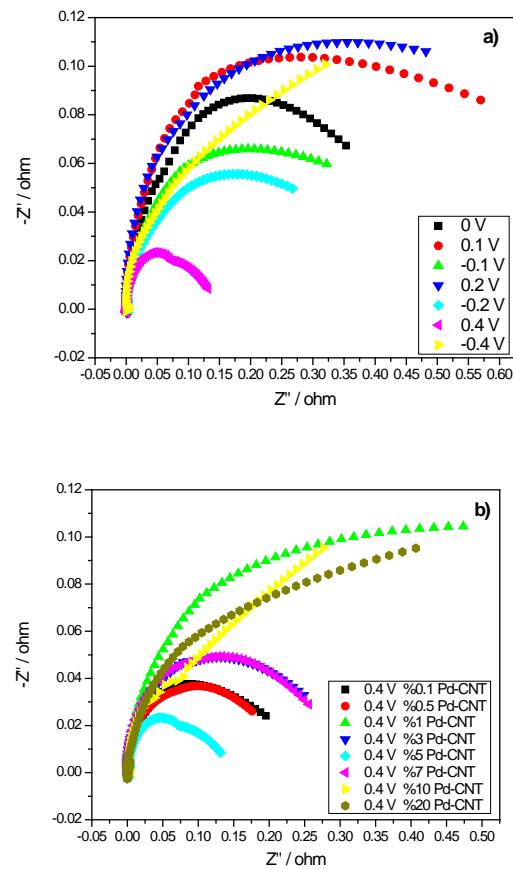


Figure 5. Nyquist Plots obtained in 1 M KOH + 0.5 M N₂H₄ solution for electrodes modified with a) 5% Pd/CNT at different potentials and b) Pd/CNT catalysts at 0.4 V.

4. Conclusion

In this study, monometallic Pd/CNT supported catalysts were prepared via the NaBH₄ reduction method. These monometallic catalysts were characterized with advance surface characterization techniques as N₂ adsorption-desorption, XRD, XPS, and TEM. To investigate their hydrazine electrooxidation activities, electrochemical techniques as CV and EIS were employed. Among the Pd/CNT catalysts, 5% Pd/CNT catalyst showed the best performance in hydrazine electrooxidation. As a result, hydrazine electrooxidation measurements and characterization conclusions of these catalysts led the following results and insights:

- 5% Pd/CNT catalyst exhibited V-type adsorption-desorption shape with H1 type hysteresis loop, which is close to the mesoporous pore structure. This result indicates that 5% Pd/CNT catalyst has a large surface area.
- The average particle size of 5% Pd/CNT catalyst from XRD was determined as 6.94 nm. In addition, the average particle size from TEM for 5% Pd/CNT catalyst was obtained as 5.17 nm. It shows that XRD and TEM average particle sizes are close.
- 5% Pd/CNT catalyst, according to CV and EIS results, displayed the highest hydrazine electrooxidation activity and long term stability compared to other Pd/CNT catalysts in hydrazine electrooxidation reaction.
- This study is unique in terms of evaluating the effect of hydrazine electrooxidation in an alkaline medium.
- Pd/CNT catalysts are promising as anode catalysts for direct hydrazine fuel cells

Acknowledgment

O. F. Er thank to the council of higher education (YOK) for 100/2000 scholarship and the Scientific and Technological Research Council of Turkey (TUBITAK) for 2211-A scholarship.

References

- [1]. Er O.F., Caglar A., Ulas B., Kivrak H., Kivrak A., "Novel carbon nanotube supported Co@ Ag@ Pd formic acid electrooxidation catalysts prepared via sodium borohydride sequential reduction method", *Materials Chemistry and Physics*, 241, (2020), 122422.
- [2]. Ellis M.W., Von Spakovsky M.R., Nelson D.J., "Fuel cell systems: efficient, flexible energy conversion for the 21st century", *Proceedings of the IEEE*, 89, (2001), 1808-1818.
- [3]. Armeanu D.Ş., Gherghina Ş.C., Pasmangiu G., "Exploring the causal nexus between energy consumption, environmental pollution and economic growth: Empirical evidence from central and Eastern Europe", *Energies*, 12, (2019), 3704.
- [4]. Ulas B., Caglar A., Sahin O., Kivrak H., "Composition dependent activity of PdAgNi alloy catalysts for formic acid electrooxidation", *Journal of colloid and interface science*, 532, (2018), 47-57.
- [5]. Kivrak H., Atbas D., Alal O., Çögenli M.S., Bayrakceken A., Mert S.O., Sahin O., "A complementary study on novel PdAuCo catalysts: Synthesis, characterization, direct formic acid fuel cell application, and exergy analysis", *International Journal of Hydrogen Energy*, 43, (2018), 21886-21898.
- [6]. Sahin O., Duzenli D., Kivrak H., "An ethanol electrooxidation study on carbon-supported Pt-Ru nanoparticles for direct ethanol fuel cells", *Energy Sources, Part A: Recovery, Utilization, and Environmental Effects*, 38, (2016), 628-634.
- [7]. Kivrak H.D., "The effect of temperature and concentration for methanol electrooxidation on Pt-Ru catalyst synthesized by microwave assisted route", *Turkish Journal of Chemistry*, 39, (2015), 563-575.
- [8]. Huynh T.T.K., Tran T.Q.N., Yoon H.H., Kim W.-J., Kim I.T., "AgNi@ ZnO nanorods grown on graphene as an anodic catalyst for direct glucose fuel cells", *Korean Journal of Chemical Engineering*, 36, (2019), 1193-1200.
- [9]. Ulas B., Caglar A., Kivrak A., Kivrak H., "Atomic molar ratio optimization of carbon nanotube supported PdAuCo catalysts for ethylene glycol and methanol electrooxidation in alkaline media", *Chemical Papers*, 73, (2019), 425-434.
- [10]. Wang Y., Wang Q., Wan L.-Y., Han Y., Hong Y., Huang L., Yang X., Wang Y., Zaghbi K., Zhou Z., "KOH-doped polybenzimidazole membrane for direct hydrazine fuel cell", *Journal of Colloid and Interface Science*, 563, (2020), 27-32.
- [11]. Granot E., Filanovsky B., Presman I., Kuras I., Patolsky F., "Hydrazine/air direct-liquid fuel cell based on nanostructured copper anodes", *Journal of Power Sources*, 204, (2012), 116-121.
- [12]. Yamada K., Asazawa K., Yasuda K., Ioroi T., Tanaka H., Miyazaki Y., Kobayashi T., "Investigation of PEM

- type direct hydrazine fuel cell”, *Journal of power sources*, 115, (2003), 236-242.
- [13]. Yi Q., Chu H., Tang M., Zhang Y., Liu X., Zhou Z., Nie H., “A novel membraneless direct hydrazine/air fuel cell”, *Fuel cells*, 14, (2014), 827-833.
- [14]. Burshtein T.Y., Farber E.M., Ojha K., Eisenberg D., “Revealing structure–activity links in hydrazine oxidation: doping and nanostructure in carbide–carbon electrocatalysts”, *Journal of Materials Chemistry A*, 7, (2019), 23854-23861.
- [15]. Yin W.X., Li Z.P., Zhu J.K., Qin H.Y., “Effects of NaOH addition on performance of the direct hydrazine fuel cell”, *Journal of power sources*, 182, (2008), 520-523.
- [16]. Crisafulli R., de Barros V.V.S., de Oliveira F.E.R., de Araújo Rocha T., Zignani S., Spadaro L., Palella A., Dias J.A., Linares J.J., “On the promotional effect of Cu on Pt for hydrazine electrooxidation in alkaline medium”, *Applied Catalysis B: Environmental*, 236, (2018), 36-44.
- [17]. Wang W., Wang Y., Liu S., Yahia M., Dong Y., Lei Z., “Carbon-supported phosphatized CuNi nanoparticle catalysts for hydrazine electrooxidation”, *International Journal of Hydrogen Energy*, 44, (2019), 10637-10645.
- [18]. Liang B., Wang Y., Liu X., Tan T., Zhang L., Wang W., Nickel–cobalt alloy doping phosphorus as advanced electrocatalyst for hydrazine oxidation, *Journal of Alloys and Compounds*, 807, (2019), 151648.
- [19]. Wang T., Wang Q., Wang Y., Da Y., Zhou W., Shao Y., Li D., Zhan S., Yuan J., Wang H., “Atomically Dispersed Semimetallic Selenium on Porous Carbon Membrane as an Electrode for Hydrazine Fuel Cells”, *Angewandte Chemie*, 131, (2019), 13600-13605.
- [20]. Liu X., Li Y., Chen N., Deng D., Xing X., Wang Y., “Ni₃S₂@ Ni foam 3D electrode prepared via chemical corrosion by sodium sulfide and using in hydrazine electro-oxidation”, *Electrochimica Acta*, 213, (2016), 730-739.
- [21]. Li C., Li M., Bo X., Yang L., Mtukula A.C., Guo L., “Facile synthesis of electrospinning Mn₂O₃-Fe₂O₃ loaded carbon fibers for electrocatalysis of hydrogen peroxide reduction and hydrazine oxidation”, *Electrochimica Acta*, 211, (2016), 255-264.
- [22]. Lao S.J., Qin H.Y., Ye L.Q., Liu B.H., Li Z.P., “A development of direct hydrazine/hydrogen peroxide fuel cell”, *Journal of Power Sources*, 195, (2010), 4135-4138.
- [23]. Raof J.B., Ojani R., Jamali F., Hosseini S.R., “Electrochemical detection of hydrazine using a copper oxide nanoparticle modified glassy carbon electrode”, *Caspian Journal of Chemistry*, 1, (2012), 73-85.
- [24]. Lin X., Wen H., Zhang D.-X., Cao G.-X., Wang P., “Highly dispersed nickel nitride nanoparticles on nickel nanosheets as an active catalyst for hydrazine electrooxidation”, *Journal of Materials Chemistry A*, 8, (2020), 632-638.
- [25]. Zabielaite A., Balčiūnaitė A., Šimkūnaitė D., Lichušina S., Stalnionienė I., Šimkūnaitė-Stanynienė B., Naruškevičius L., Tamašauskaitė-Tamašiūnaitė L., Norkus E., Selskis A., “High Performance Direct N₂H₄-H₂O₂ Fuel Cell Using Fiber-Shaped Co Decorated with Pt Crystallites as Anode Electrocatalysts”, *Journal of The Electrochemical Society*, 167, (2020), 054502.
- [26]. Wen H., Cao G.-X., Chen M.-H., Qiu Y.-P., Gan L.-Y., Wang P., “Surface phosphorization of hierarchically nanostructured nickel molybdenum oxide derived electrocatalyst for direct hydrazine fuel cell”, *Applied Catalysis B: Environmental*, 268, (2020), 118388.
- [27]. Lei Y., Liu Y., Fan B., Mao L., Yu D., Huang Y., Guo F., “Facile fabrication of hierarchically porous Ni foam@ Ag-Ni catalyst for efficient hydrazine oxidation in alkaline medium”, *Journal of the Taiwan Institute of Chemical Engineers*, 105, (2019), 75-84.
- [28]. Yang G.-W., Gao G.-Y., Wang C., Xu C.-L., Li H.-L., “Controllable deposition of Ag nanoparticles on carbon nanotubes as a catalyst for hydrazine oxidation”, *Carbon*, 46, (2008), 747-752.
- [29]. Gao H., Wang Y., Xiao F., Ching C.B., Duan H., “Growth of copper nanocubes on graphene paper as free-standing electrodes for direct hydrazine fuel cells”, *The Journal of Physical Chemistry C*, 116, (2012), 7719-7725.
- [30]. Asset T., Roy A., Sakamoto T., Padilla M., Matanovic I., Artyushkova K., Serov A., Maillard F., Chatenet M., Asazawa K., “Highly active and selective nickel molybdenum catalysts for direct hydrazine fuel cell”, *Electrochimica Acta*, 215, (2016), 420-426.

- [31]. Liu W., Xie J., Guo Y., Lou S., Gao L., Tang B., "Sulfurization-induced edge amorphization in copper–nickel–cobalt layered double hydroxide nanosheets promoting hydrazine electro-oxidation", *Journal of Materials Chemistry A*, 7, (2019), 24437-24444.
- [32]. Chen L.-X., Jiang L.-Y., Wang A.-J., Chen Q.-Y., Feng J.-J., "Simple synthesis of bimetallic AuPd dendritic alloyed nanocrystals with enhanced electrocatalytic performance for hydrazine oxidation reaction", *Electrochimica Acta*, 190, (2016), 872-878.
- [33]. Zhao A., Sun H., Chen L., Huang Y., Lu X., "Development of highly efficient and scalable free-standing electrodes for the fabrication of hydrazine-O₂ fuel cell", *Materials Research Express*, 6, (2019), 085533.
- [34]. Akbar K., Kim J.H., Lee Z., Kim M., Yi Y., Chun S.-H., "Superaerophobic graphene nano-hills for direct hydrazine fuel cells", *NPG Asia Materials*, 9, (2017), e378-e378.
- [35]. Yan X., Meng F., Xie Y., Liu J., Ding Y., "Direct N₂ H₄/H₂O₂ fuel cells powered by nanoporous gold leaves", *Scientific reports*, 2, (2012), 941.
- [36]. Ding J., Kannan P., Wang P., Ji S., Wang H., Liu Q., Gai H., Liu F., Wang R., "Synthesis of nitrogen-doped MnO/carbon network as an advanced catalyst for direct hydrazine fuel cells", *Journal of Power Sources*, 413, (2019), 209-215.
- [37]. Sing K.S., Williams R.T., "Physisorption hysteresis loops and the characterization of nanoporous materials", *Adsorption Science & Technology*, 22, (2004), 773-782.
- [38]. Kivrak H., Alal O., Atbas D., "Efficient and rapid microwave-assisted route to synthesize Pt–MnOx hydrogen peroxide sensor", *Electrochimica acta*, 176, (2015), 497-503.
- [39]. Chen N., Deng D., Li Y., Liu X., Xing X., Xiao X., Wang Y., "TiO₂ nanoparticles functionalized by Pd nanoparticles for gas-sensing application with enhanced butane response performances", *Scientific reports*, 7, (2017), 7692.
- [40]. Lin J., Mei T., Lv M., Zhang C.A., Zhao Z., Wang X., "Size-controlled PdO/graphene oxides and their reduction products with high catalytic activity", *RSC Advances*, 4, (2014), 29563-29570.
- [41]. Wepasnick K.A., Smith B.A., Bitter J.L., Fairbrother D.H., "Chemical and structural characterization of carbon nanotube surfaces", *Analytical and bioanalytical chemistry*, 396, (2010), 1003-1014.
- [42]. Qi B., Di L., Xu W., Zhang X., "Dry plasma reduction to prepare a high performance Pd/C catalyst at atmospheric pressure for CO oxidation", *Journal of Materials Chemistry A*, 2, (2014), 11885-11890.
- [43]. Caglar A., Kivrak H., "Highly active carbon nanotube supported PdAu alloy catalysts for ethanol electrooxidation in alkaline environment", *International Journal of Hydrogen Energy*, 44, (2019), 11734-11743.
- [44]. Eshghi A., "Graphene/Ni–Fe layered double hydroxide nano composites as advanced electrode materials for glucose electro oxidation", *International Journal of Hydrogen Energy*, 42, (2017), 15064-15072.
- [45]. Qu W., Wang Z., Sui X., Gu D., "An efficient antimony doped tin oxide and carbon nanotubes hybrid support of Pd catalyst for formic acid electrooxidation", *international journal of hydrogen energy*, 39, (2014), 5678-5688.